Journal of Non-Crystalline Solids 355 (2009) 1119–1122

Contents lists available at ScienceDirect

Journal of Non-Crystalline Solids

journal homepage: www.elsevier.com/locate/jnoncrysol

Time-resolved photoluminescence of implanted SiO_2:Si^+ films

A.F. Zatsepin [a], V.A. Pustovarov [a], V.S. Kortov [a], E.A. Buntov [a,*], H.-J. Fitting [b]

[a] Ural State Technical University–UPI, 19 Mira St., 620002 Ekaterinburg, Russia
[b] Institute of Physics, University of Rostock, Universitätsplatz 3, D-18051 Rostock, Germany

ARTICLE INFO

Article history:
Available online 14 May 2009

PACS:
78.47.Cd
71.35.−y
78.67.Hc
78.66.−w

Keywords:
Films and coatings
Optical spectroscopy
Defects
Nanoparticles
Colloids and quantum structures
Luminescence
Time resolved measurements
Silica

ABSTRACT

In this paper we present results of a low-temperature time-resolved photoluminescence (PL) investigation of thin SiO_2 films implanted with silicon ions. In addition to the luminescence of well-known ODCs, some other bands are present in the low-energy region of PL spectra that are attributed to silicon nanoclusters (quantum dots – SiQDs), excitons and hydrogen-related species (HRS). Specific features of SiQD and HRS bands are the nanosecond kinetics and unusual "stepped" PL excitation spectrum in the 3.5–7.5 eV range. The possible origin of discovered phenomena is discussed. The obtained results are interpreted taking into account the interference of exciting radiation and dimensional quantization effects.

1. Introduction

The need for optoelectronic devices which can be integrated into the current Si technology has initiated an intense research for silicon-based light emitters. Among different approaches the Si-implanted SiO_2 is a very promising material. Due to its full compatibility with state-of-the-art Si technology, the very good control over the fabrication process, ion implantation into SiO_2 appears to be one of the most suitable fabrication methods for these purposes. Incorporating of nano-sized silicon particles in a SiO_2 matrix ensures stability of such materials.

Application of those to commercial devices requires deeper knowledge of their energy band structures; in particular, the information related to the electronic properties of the impurity atoms and defect states. During past decade, noted properties have been widely studied for their luminescence and charge retention properties (see, for instance, [1–5]). Despite some success achieved the mechanism of light emission from implanted Si/SiO_2 layers is more complicated and still unclear.

On the one hand the blue–violet photoluminescence of SiO_2 is generally believed to be caused by oxygen-deficient centers [6]. Recently another yellow luminescence band (2.15 eV) is reported in literature [1,2] which was not studied intensively. On the other hand the strong confinement of silicon nanocrystals (Si-nc) may improve the radiative probability of silicon and shifts the emitted spectral band to the visible range [3]. Finally, the active role of the "Si-nc/a-SiO_2" interface is highlighted as its quality and stability were found to be responsible for the optical properties of the systems with Si-nanocrystals [4,5].

Recently we studied specific features of the photoluminescence of oxygen-deficient centers in nanostructured silicon dioxide as well as the time-resolved photoluminescence of SiO_2 layers implanted with Ge^+ ions [7,8]. Steady-state cathodoluminescence properties of such layers were studied in [9,10]. The present study is concerned with radiative relaxation processes involving photosensitive defects and nanoclusters in SiO_2 films implanted with Si^+ ions. Selective photoexcitation together with time-resolved photoluminescence registration allow us to investigate the spectral-kinetic features of point defects and nanoclusters under intracenter excitation. Such method may help us answer the aforementioned questions concerning Si–SiO_2 luminescence features.

2. Objects and experimental procedures

Time-resolved photoluminescence (PL) spectra in the region of 1.3–6.0 eV, time-resolved PL excitation spectra (3.7–19.0 eV), and the PL decay kinetics were measured using synchrotron radiation

* Corresponding author. Tel.: +7 9086312122.
E-mail addresses: buntov@dpt.ustu.ru, fmpk_john@mail.ru (E.A. Buntov).

0022-3093/$ - see front matter © 2009 Elsevier B.V. All rights reserved.
doi:10.1016/j.jnoncrysol.2009.01.048

(SR) on a SUPERLUMI station (Beam-line I, HASYLAB, DESY). The 0.3 m ARC Spectra Pro-300i monochromator and either an R6358P (Hamamatsu) photomultiplier or a CCD camera were used as the registration system. The absolute error of spectral position determination was less than 0.03 eV while the intensity error due to noise and source instability was not more than 5%. Time-resolved PLE spectra were measured in two time spans $\Delta t_1 = 21$ ns (the fast component) and $\Delta t_2 = 72$ ns (the slow component), which were delayed relative to the beginning of the SR-excitation pulse for $\delta t_1 = 3.7$ ns and $\delta t_2 = 101$ ns respectively. The excitation spectra were normalized to the same number of SR-exciting photons using sodium salicylate. PL decay kinetics was measured under 3 ns SR-excitation pulses separated by 192 ns interpulse distance. The convolution method was used to analyze the PL decay. All the measurements were made at $T = 9$ K. As samples we have used amorphous, thermally grown SiO_2 layers, 500 nm thick, wet oxidized at 1100 °C on a crystalline Si substrate. The layers were of microelectronic quality. The ion implantations of Si^+ were performed with energy of 150 keV, with a uniform dose of 5×10^{16} ions/cm^2. This implantation energy and dose led to an atomic dopant fraction of about 4 at.% at nearly the half depth of the oxide layers. The implantation and depth profiling processes were described in details elsewhere [9,11]. A post-implantation thermal annealing was performed at temperature $T_a = 900$ °C for 1 h in dry nitrogen.

3. Results

The PL spectra of the implanted films are dominated at room temperature by the luminescence of the known α-ODC and β-ODC with the radiative transitions at 2.7; 4.5 eV and 3.1; 4.3 eV, respectively. Each type of defects is responsible for two PL bands which are connected with singlet–singlet and triplet–singlet transitions. Observed ODCs have a characteristic PL excitation spectrum (the maximum near 5.0–5.15 eV). Post-implantation annealing does not change parameters of the observed PL of ODCs. The shape of the low-temperature PL spectra of annealed samples changed considerably in other spectral regions. Time-integrated PL spectra obtained at different energies of excitation photons are shown in Fig. 1. The non-elementary 4.5 eV PL band corresponding to the singlet luminescence of α-ODC (4.3 eV) and β-ODC (4.5 eV) [6], as well as an unidentified peak near 3.6 eV are observed under 5.1 eV excitation. The growth of the luminescence intensity near 3.1 eV is assumed to be due to the presence of the ODC triplet radiation. The intensity of the triplet PL bands is quite low because of the activation barrier for the transfer of the excitation energy between the singlet and triplet states. Also, some new peaks appear in the PL spectrum in the long-wavelength region at energies of 1.34, 1.72, 1.9, 2.18, and 2.58 eV. The shape of the PL spectrum depends on the energy of excitation photons. As regards their location, the bands at 1.7 and 1.9 eV can be referred to surface and bulk types of non-bridging oxygen hole centers (NBOHCs) [11,3]. The maxima at 2.18 and 2.58 eV can presumably be related to either the luminescence of silicon nanoclusters or hydrogen-related species [12].

Figs. 2 and 3 present time-resolved excitation spectrum of 2.81 eV band and steady-state excitation spectra of different PL bands respectively. The excitation spectra have a complicated "stepped" shape and include a set of relatively sharp bands in the low-energy region ($h\nu_{exc} = 4.45$; 5.14; 5.88; 6.45; 6.96 eV, FWHM is about 0.5 eV) and a wider band (FWHM near 2 eV) in the region of 8–10 eV. All these peaks cannot be attributed to some type of ODCs. Moreover, the wide band at 7.75 eV corresponds to the region of the exciton generation and the edge of the interband transitions region for the SiO_2 matrix. The positions of the maximum, FWHM and the relative integral intensity of all the bands are almost the same for each of the three PL peaks, see Table 1.

To investigate the nature of the discovered luminescence, we performed a set of kinetic measurements. Time-resolved lumines-

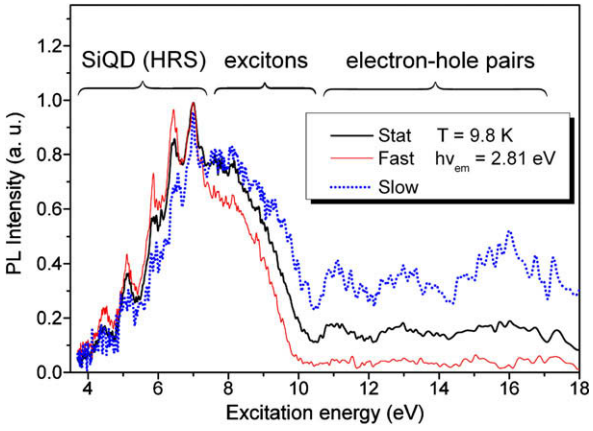

Fig. 2. Time-resolved PL excitation spectra of the 2.81 eV emission band in a SiO_2:Si^+ film.

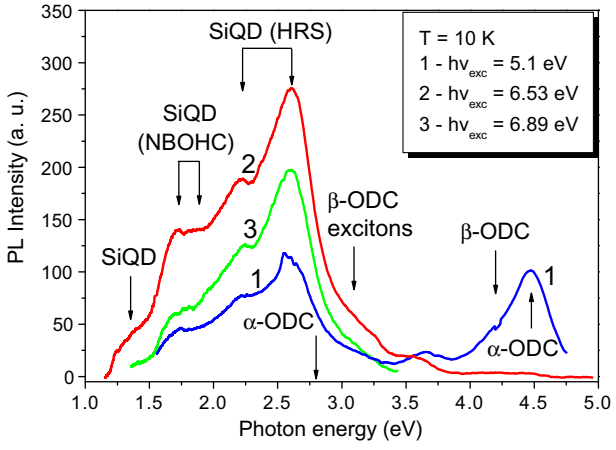

Fig. 1. Time-integrated PL spectra of a SiO_2:Si^+ film at $E_{exc} = 5.10$ eV (1), 6.53 eV (2) and 6.89 eV (3) recorded by a CCD camera.

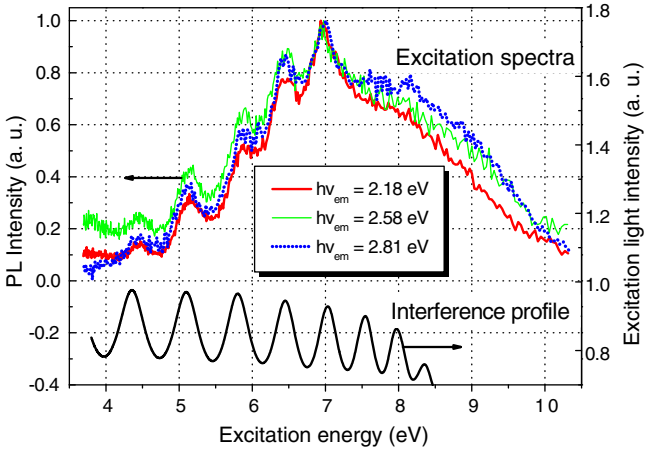

Fig. 3. Time-integrated PL excitation spectra of 2.81, 2.58 and 2.18 eV emission bands in a SiO_2:Si^+ film and the interference profile calculated for this film.

Table 1
Positions of maxima E_{max}, *FWHM* and the integral intensity *S* of sub-bands in "stepped" PL excitation spectra.

E_{max} (eV)	4.40	5.14	5.86	6.42	6.96	7.58
FWHM (eV)	0.53	0.33	0.42	0.34	0.45	3.16
S (a.u.)	0.052 ± 0.003	0.066 ± 0.003	0.096 ± 0.005	0.11 ± 0.01	0.16 ± 0.01	2.3 ± 0.1

Note: E_{max} and *FWHM* were determined with maximum error 0.03 eV.

cence excitation spectra over a wide spectral range and a series of decay kinetics curves for different PL bands at different excitation energies were recorded (Figs. 2, 4 and 5). Time-resolved spectra demonstrate different radiative relaxation kinetics for various regions of the excitation energy. The normalized fast component dominates over the slow component on the low-energy side of the spectrum, while their ratio reverses at 7–20 eV. The difference in the PL decay kinetics points to the corresponding difference in PL excitation mechanisms for these centers. This conclusion agrees well with results of direct kinetic measurements, see Figs. 4 and 5. The decay kinetics of the PL band at 2.53 eV can be approximated well by two exponents with the average decay times of 4.5 and 35 ns respectively. Lifetimes almost do not depend on excitation energy (Fig. 4). At the same time emission band strongly influences

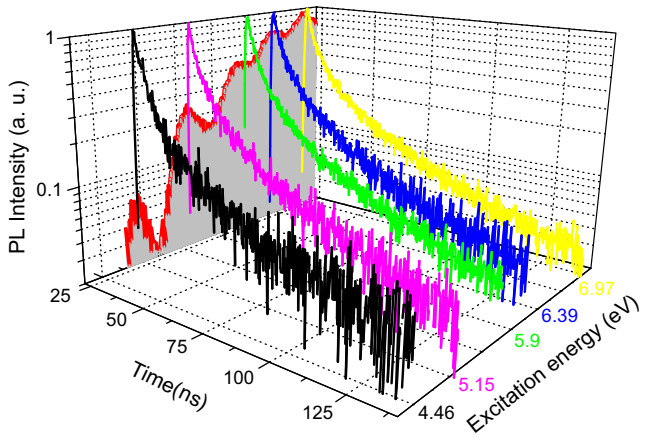

Fig. 4. PL decay kinetics of the 2.53 eV emission band in a SiO_2:Si^+ sample on the semilogarithmic scale. The PL excitation spectra (the red dashed line) are given for reference. (For interpretation of the references to color in this figure legend, the reader is referred to the web version of this article.)

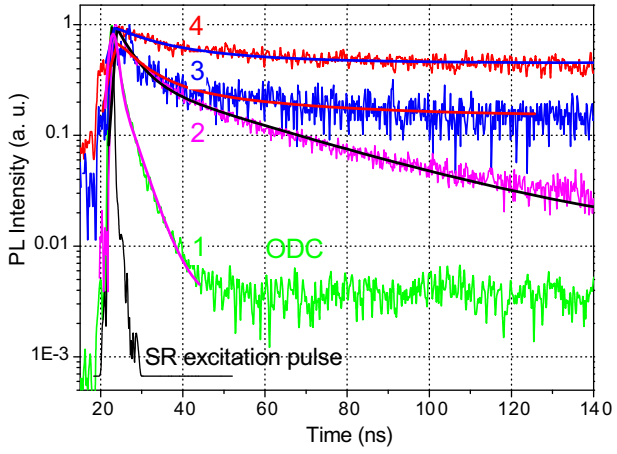

Fig. 5. PL decay kinetics of 4.37 (1, $h\nu_{exc}$ = 5.0 eV), 2.53 eV(2), 2.14 eV (3) and 1.72 eV (4) emission bands at $h\nu_{exc}$ = 6.97 eV in SiO_2:Si^+ films.

decay kinetics (Fig. 5). The 2.14 eV band has the same order of the decay time: 6.5 and 50 ns. At the same time the PL kinetics in both bands slow down at high excitation energies near 8 eV (6 and 43 ns for $h\nu_{em}$ = 2.53 eV; 7 and 55 ns for $h\nu_{em}$ = 2.14 eV). The third PL band at 1.72 eV has the maximum decay time: 8, 50 ns and components of the μs range.

4. Discussion

Although the observed ODCs (Fig. 1) have been intensively studied, there is no common viewpoint concerning their nature. Detailed discussion of this topic goes beyond the scope of the present article. However we should give a brief description of interpretations proposed in literature. The first explanation of noted bands is as a point defect such as an oxygen vacancy or a relaxed ≡Si—Si≡ (α-ODC) and ≡Ge—Ge≡ (β-ODC) bonds (see, for example, [13]). Our previous investigation has shown that there could be even more types of oxygen-deficient centers contributing to 2.7–3.2 eV and 4.2–4.5 eV PL [14]. The second approach ascribes them to twofold silicon and germanium atoms respectively [6,15,16]. Moreover, in the present case we cannot confidently propose germanium-related models of ODCs as Ge atoms were not deliberately introduced into silica matrix. In this paper we ascribe observed PL bands to some oxygen vacancy related defects.

The obtained results suggest that in addition to the well-known ODCs a specific type of defect centers is present in the SiO_2:Si^+ films under study. Parameters of the aforementioned defects are close to those of defects in nanosized modifications of SiO_2 [12]. Their specific features include an abnormally wide spectral region and a "stepped" shape of excitation spectra. Some investigators relate similar centers to a specific type of defects (so-called Hydrogen-Related Species – HRS) observed in amorphous SiO_2 nanoparticles [12].

In our opinion, these results can be interpreted as outlined below. On the one hand, a specific shape of the excitation spectra may be due to size effects because of silicon nanoclusters (quantum dots) formed during post-implantation annealing of the SiO_2 matrix. The observed "stepped" spectrum can result from dimensional quantization of the density of electron states. It reflects the presence of a system of discrete energy levels [17]. At the same time, the phenomenon of interference can play some role in this case. The effect of the interference of the luminescence radiation in analogous materials was studied in [18,19]. In this work we used a program [20] and calculated the distribution of the electrical component intensity in the field of an incident light wave taking into account the experimental conditions (the film 500 nm thick, the incident angle of the excitation radiation being 17 degrees, and the spectrum range of 4–8.5 eV). Parameters of the distribution profile of implanted Si^+ ions, which were calculated using the SRIM-2006 program (the average penetration depth of 146 nm, the distribution half-width of 34 nm), were considered too. We assumed the depth distribution of silicon nanoclusters approximately coinciding with ion profile. The calculation results demonstrate that the interference of the incident and the reflected radiation can cause oscillations of the spectral distribution of the excitation light intensity (Fig. 3), which are related to the formation of standing waves in the film. In this case the position and

the width of the interference maxima approach closely the analogous parameters of the bands in the experimental spectra.

However, we cannot take the interference of excitation radiation to be the main reason for the discovered phenomena. **Why?** Firstly, it is now clear for us that this "stepped" excitation spectrum appears only after implantation. Moreover, annealing process increases its intensity. Secondly, we observed a similar "stepped" excitation spectrum earlier in implanted bulk glasses and nanocompacts, in which the interference can hardly manifest itself [21]. At last, the absence of interference oscillations in the high-energy region of the spectrum (more than 7.5 eV) is still unclear, although calculations predict a considerable decrease in their amplitude in the region of 9 eV only. This is indicative of the non-elementary nature of the spectrum and the presence of two bands (near 6.5 and 7.75 eV, respectively) corresponding to different mechanisms of the PL excitation. Thus, one may think that PL of SiO_2 films probably is characterized by a superposition of the interference profile and a characteristic "stepped" excitation spectrum resulting from the dimensional quantization of the electron states density of the interface in the "Si cluster – SiO_2 matrix" system.

One more argument in favor of this supposition is the slower kinetics of the high-energy portion of the spectrum (Fig. 3) and a redistribution of the intensity of the two portions of the excitation spectrum as the emission wavelength changes: the contribution from the high-energy excitation band at 7.75 eV grows with the emission energy. This effect may be due to the SiO_2 bound exciton luminescence, which shows up over the interval of 2.7–3.25 eV [22]. The excitation spectrum region of 10–20 eV results from interband transitions in SiO_2, which are accompanied by formation of electron-hole pairs. It should be emphasized that the PL bands at 1.34 and 1.72 eV coincide as to their energy positions with the luminescence of Si nanoclusters in the SiO_2 matrix [23,24]. In other papers the peaks between 1.3 and 1.6 eV are often related to a-SiO_2 and quantum dots, respectively [11]. Thus, their nature is still controversial and more studies need be performed for its elucidation.

5. Conclusion

The time-resolved photoluminescence measurements of Si^+ implanted and annealed SiO_2 films were performed. The following results were obtained:

Besides the luminescence of known ODCs, there are several new peaks in the 1.3–2.7 eV region that may be due to either nano-sized silicon clusters (SiQDs) or surface states of HRS type located at the "Si cluster – SiO_2 matrix" interface. The analysis of interference and other possible reasons of such spectra shows that noted spectra shape may be caused by superposition of initial "stepped" excitation spectrum of luminescent centers and the interference profile of exciting radiation.

Using time-resolved techniques we divided the excitation spectrum into three parts corresponding to three excitation mechanisms. The most slow PL decay kinetics (μs range components) is characteristic for excitons and generation of electron-hole pairs due to recombination processes taking place in this case. The specific features of PL maxima ascribed to SiQDs or HRS are the characteristic multiband structure of the excitation spectra and the nanosecond decay kinetics that is independent of exciting photons energy within the 4–7.5 eV range.

Acknowledgements

This work was partially supported by the Russian Education Agency (Program "The development of scientific potential of higher school 2006-08", project 2948) and RFBR (Grant 08-02-01072).

References

[1] Y.D. Glinka, S.-H. Lin, Y.-T. Chen, Phys. Rev. B 66 (2002) 035404.
[2] C. Mühlig, S. Kufert, W. Triebel, F. Coriand, Proc. Int. Soc. Opt. Eng. SPIE 4779 (2003) 107.
[3] T. Shimizu-Iwayama, N. Kurumado, D.E. Hole, P.D. Townsend, J. Appl. Phys. 83 (1998) 6018.
[4] N. Daldosso et al., Phys. Rev. B 68 (2003) 085327.
[5] K.S. Zhuravlev, A.M. Gilinsky, A.Yu. Kobitsky, Appl. Phys. Lett. 73 (1998) 2962.
[6] L.N. Skuja, J. Non-Cryst. Solids 239 (1998) 16.
[7] V.S. Kortov, A.F. Zatsepin, V.A. Pustovarov, A.A. Chudinov, D.Yu. Biryukov, Radiat. Meas. 42 (2007) 891.
[8] V.A. Pustovarov, A.F. Zatsepin, D.Yu. Biryukov, V.S. Kortov, B. Schmidt, Roushdey Salh, H.-J. Fitting, HASYLAB Annual Report (2005) 707.
[9] H.-J. Fitting, T. Barfels, A.N. Trukhin, B. Schmidt, A. Gulans, A. von Czarnowski, J. Non-Cryst. Solids 303 (2002) 218.
[10] A.N. Trukhin, J. Jansons, H.-J. Fitting, T. Barfels, B. Schmidt, J. Non-Cryst. Solids 331 (2003) 91.
[11] Roushdey Salh, A. von Czarnowski, M.V. Zamoryanskaya, E.V. Kolesnikova, H.-J. Fitting, Phys. Stat. Sol. (a) 203 (2006) 2049.
[12] Yu.D. Glinka, S.-H. Lin, Y.-T. Chen, Appl. Phys. Lett. 75 (1999) 6.
[13] H. Hosono, Instrum. Meth. Phys. Res. B 65 (1992) 375.
[14] A.F. Zatsepin, H.-J. Fitting, V.S. Kortov, V.A. Pustovarov, B. Schmidt, E.A. Buntov, J. Non-Cryst. Solids 355 (2009) 61.
[15] A.N. Trukhin, H.-J. Fitting, J. Non-Cryst. Solids 248 (1999) 49.
[16] M. Cannas, S. Agnello, R. Boscaino, F.M. Gelardi, S. Grandi, P.C. Mustarelli, J. Non-Cryst. Solids 322 (2003) 129.
[17] J.M. Martinez-Duart, R.J. Martin-Palma, F. Agullo-Rueda, Nanotechnology for Microelectronics and Optoelectronics, Elsevier, 2006.
[18] R. Smirania, F. Martina, G. Abela, Y.Q. Wanga, M. Chicoineb, G.G. Ross, J. Lumin. 115 (2005) 62.
[19] G.G. Ross, D. Barbaa, C. Dahmounea, Y.Q. Wanga, F. Martin, Instrum. Meth. Phys. Res. B 256 (2007) 211.
[20] D.L. Windt, Comput. Phys. 12 (1998) 360.
[21] A.F. Zatsepin, V.S. Kortov, N.V. Gavrilov, D.Yu. Biryukov, J. Surf. Invest.: X-ray, Synchrotron Neutron Tech. 2 (2008) 450.
[22] Yuri D. Glinka, Phys. Rev. B 66 (2002) 035404.
[23] O.N. Gorshkov, Yu.A. Dudin, V.A. Kamin, A.P. Kasatkin, A.N. Mikhaylov, V.A. Novikov, D.I. Tetelbaum, Tech. Phys. Lett. 31 (2005) 509.
[24] A.V. Sachenko, Yu.V. Kryuchenko, I.O. Sokolovskii, O.M. Sreseli, Semiconductors 38 (2004) 842.